

Numerical Simulation of Ductile Fracture Process including Shear-Lip Fracture

M. Kikuchi¹ and S. Sannoumaru²

Summary

Thickness effect is studied experimentally. At free surface of the specimen, shear lip fracture pattern appears, though dimple fracture pattern is observed inside of the specimen. The area of shear-lip fracture changes due to the change of the specimen thickness. In this study, experimental study is conducted by changing specimen thicknesses. Fracture surfaces are precisely observed using SEM, and dimple patterns on them are observed. At the free surface, very narrow no-void area is observed. By using FRASTA technique, dimple fracture process is simulated. It is found that shear-lip fracture appears after dimple fracture process. FEM simulation is carried out using Gurson's constitutive equation. It is found that shear-lip type fracture is simulated near free surface area by this method. The results show similar tendency with the experimental observation.

Introduction

In the elastic-plastic fracture mechanics, J integral concept [1] is considered to be one of the most important parameters, which controls the fracture process in the crack tip process zone. But by many experimental studies, it has been shown that the apparent J integral value changes due to the change of the constraint condition at the crack tip [2,3]. It is called constraint effect. Many studies have been conducted on the effect of the constraint [4-6]. Thickness effect is one of constraint effect problems. This is due to the plane stress state at the free surface of cracked plate. Conventional fracture mechanics mainly considers fracture under plane strain stress state. To satisfy the plane strain stress condition, thickness is determined in the J integral testing standard [7]. But as the machine becomes small, thin plate is used and plane stress state is not neglected. Under plane stress state, shear-lip fracture occurs, though dimple fracture is observed under plane strain condition. The mechanics of shear-lip fracture has not been studied well yet[8,9]. In this study, shear-lip fracture is precisely studied experimentally. Then the dimple fracture process is simulated numerically using Gurson's constitutive equation. Numerical results are compared with those of experiments, and the effect of shear-lip zone on fracture process is discussed.

Experiments

Three point bend specimen, as shown in Figure 1, is used for ductile fracture test. The material of this specimen is A533B steel, which is used for pressure vessel of Nuclear Power Plant. Mechanical properties and chemical compositions of

¹Dept. Mech. Engng., Tokyo University of Science, Japan

²Graduation School of Tokyo University of Science, Japan

this material are shown in Table 1 and Table 2. By the fracture toughness testing standard [7], the minimum thickness of this specimen is 7mm. In the experiment, thickness B of the specimen is changed in three cases, 2mm, 4mm and 8mm, respectively. Dimple fracture tests are conducted by static loading. For each specimen, three specimens are tested.

Table 1: Chemical Component Of A533B Steel

C	Si	Mn	P	S	Ni	Mo
0.22	0.32	1.46	0.01	0.01	0.60	0.57

Table 2: Mechanical Property of A533B Steel

Young's modulus	Yield stress	Tensile strength
E	σ_{ys}	σ_B
206[GPa]	599[MPa]	720[MPa]

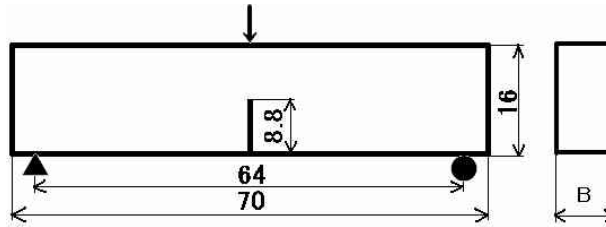


Figure 1: Three point bend specimen

Fracture surface observation

Fracture surface is observed after dimple fracture test. Figure 2 is a fracture surface of 8mm thick specimen. At both surface, shear-lip fracture areas are observed, and dimple fracture area appears in flat area inside of the specimen. Using SEM(Scanning Electron Microscope), fracture surface is observed in detail along a line shown in Figure 2. As the results, three kinds of characteristic fracture patterns are observed as shown in Figure 3. Figure 3 (a) shows very flat fracture surface, where no voids are observed. It exists very near to the specimen surface. This area is called pattern I. A little inside from the specimen surface, many small voids are observed as shown in Figure 3 (b). This area exists in shear-lip zone. This is called pattern II. At the center part of the specimen, large voids are observed as shown in Figure 3(c). This area is dimple fracture zone, which occurs under plane strain condition. It is called pattern III.

The ratios of the width of pattern I and II (they are called WI and WII, respectively) to specimen thickness, B, are measured and results are shown in Table 3. As the specimen thickness decreases, the ratio of WII/B increases. It is reasonable because plane stress state area increases by the decrease of specimen thickness. But it is interesting to note that WI/B keeps nearly constant value with the change

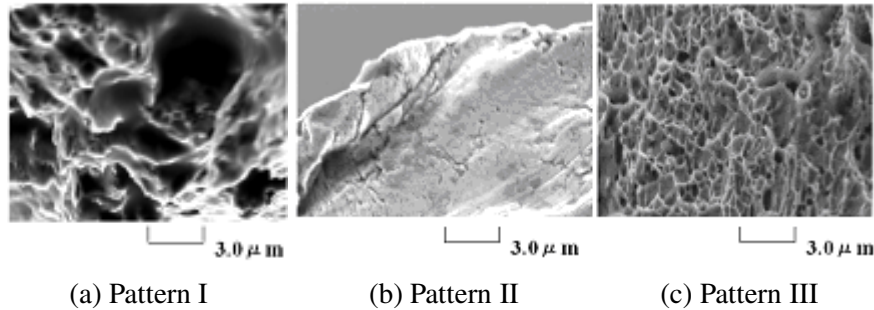
of specimen thickness. Also, these values are very small. The area of pattern I is under 1% of the whole specimen thickness. In other words, more than 99% of fracture surface is covered by voids, though shear-lip fracture area increases in thin specimen.

Table 3: WI/B and WII/B

B	2	4	8
WI/B	0.00892	0.00722	0.00682
WII/B	0.290	0.319	0.282



Figure 2: Fracture surface of three point bend specimen.

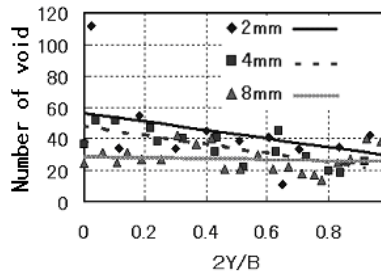
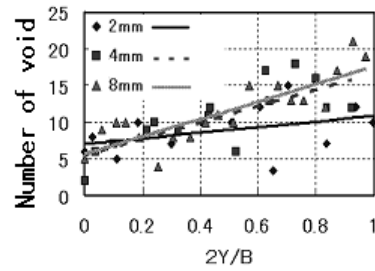


(a) Pattern I (b) Pattern II (c) Pattern III

Figure 3: Three patterns of fracture surface.

Number of voids on fracture surface is counted for each specimen. As the void size change widely, small voids are neglected. Figure 4 shows distributions of voids larger than $3\mu\text{m}$ along the crack front. In this figure, abscissa shows normalized location along the crack front. $2Y/B=0$ is specimen surface, and $2Y/B=1$ is at the mid-plane of the specimen. The distribution patterns of three specimens are nearly same with each other. It means many voids more than $3\mu\text{m}$ exist nearly equally along the crack front.

Figure 5 shows distributions of larger voids along the crack front. In this figure, voids larger than $20\mu\text{m}$ are counted. In this case, distribution patterns change clearly by the specimen thickness. In 2mm thick specimen, they exist nearly constant along the specimen thickness, and number of them is not large. But for 4mm and 8mm specimens, number of large voids increase inside of the specimen. It means that dimple fracture mode is dominant inside of thick specimen.

Figure 4: Voids larger than $3\mu\text{m}$.Figure 5: Voids larger than $20\mu\text{m}$.

Numerical Simulation

To consider the microscopic fracture process, the simulation of the nucleation, growth and coalescence of voids is needed. For this purpose, FEM analysis using constitutive equation proposed by Gurson [10] and later modified by Tvergaard [11] is conducted.

As many parameters are needed for the use of Gurson's model, they are determined based on literature [12] and by authors' study [13]. For the use of Gurson's model, the finite deformation analysis is needed. For this purpose, crossed triangle element and super-box element are used for 2-dimensional and 3-dimensional models, respectively, in FEM modeling.

Figure 6 (a)-(c) shows final fracture profile of three specimens. In these figures, left side is free surface and right side is mid-plane of specimen. Black area means fracture area. In Fig.6(a), result of 2mm thick specimen, flat fracture grows in the initial crack plane inside of the specimen. This is dimple fracture area observed in experiment. Near free surface, inclined fracture area grows along shear stress direction. This is a typical feature of shear-tip fracture observed experimentally. This inclined area becomes smaller as the specimen thickness increases, as shown in Fig. 6(b) and (c). Flat fracture area increases for thick specimen. These results are very similar to experimental ones.

In these numerical simulations void growth is assumed to be due to two factors. One is nucleation term, and another is growth term. In Figure 6 (a)-(c), ratios of nucleation term with respect to total void volume fraction are also shown. As shown in these figures, nucleation term increases in shear-tip fracture area and decreases in dimple fracture area. It means that many small voids are nucleated in shear-tip area, but they don't grow largely. It agrees with experimental observation, shown in Figure 4.

Figure 7(a)-(c) shows distributions of stress triaxiality at final fracture of each specimen. It is shown that stress triaxiality is large inside of thick specimen. In thin specimen, it is small at mid-plane of the specimen. At free surface area, it is small for all specimens. Stress triaxiality is deeply related with dilatation of the material,

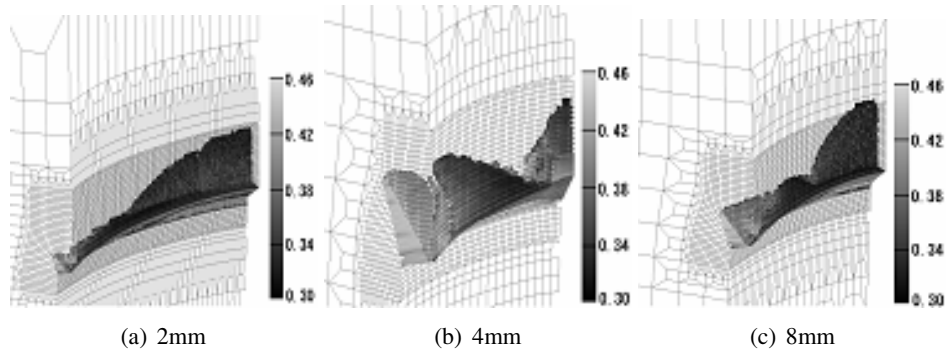


Figure 6: Final fracture zone and void nucleation term in each specimen.

and void growth is due to the dilatation of the material. It is obvious that dimple fracture is mainly due to the void growing term of void growth.

By these results, it is shown that Gurson's constitutive equation, and dimple fracture simulation method based on this equation, are available to evaluate shear-lip fracture at free surface.

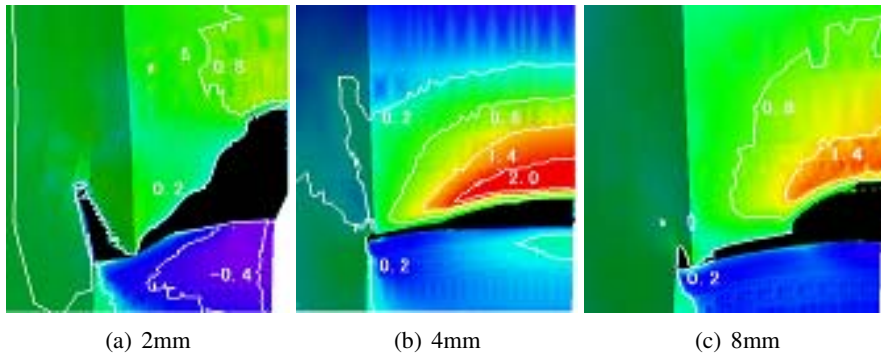


Figure 7: Distribution of stress triaxiality in each specimen

Conclusions

By experimental study, it is shown that void nucleation is deeply related with shear-lip fracture of this material. Numerical simulation also shows void growth analysis is available to evaluate both dimple and shear-lip fracture processes.

By using this numerical method, there is a possibility to evaluate thickness effect of fracture toughness, which is one of important constraint condition problems. For this purpose, it is necessary to conduct further experiments using other materials, and fracture simulation of surface crack problem, which are our next target.

References

1. Rice, J.R. (1968); Transactions. ASME, J. Applied Mechanics, vo1.90, Series E, pp.379-386

2. C.Betegon, C. Rodriguez and F.J.Belzu.nce: Fatigue Fract, Engng Mater. Struct, 20(1997), 633-644
3. Ruggieri C. and Dodds Jr.(1996) , Int. J. Fracture 79, pp.309-340.
4. Xia L. and Shih C. F. (1996): J. Mech. Phys. Solids 44, pp.603-639
5. O'Dowd N. P and Shih C. F.(1991), J. Mech. Phys. Solids 39, pp.989-1015
6. Sorensen W.A, Dodds R.H. and Rolfe S.T.: Int. J. Fracture, 47(1991), 105
7. JSME Standard S 00 1-1992 (1992), Japan Society of Mechanical Engineer
8. Koers R. W. J., Kroom A. H. M. and Bakker A, (1995): ASTM STP 1224
9. C.Betegon et al.: Fatigue Fract. Engng Mater. Struct, 20(1997), 633-644
10. Gurson, A.L.(1977); Trans. ASME, J. Engineering and-Materials, and Technology, 99, pp.2-15
11. Tvergaard. Y(1982): Int. J. Fracture 18, pp.237-252
12. Broek, D.(1973); Eng. Frac. Mech., vol.5. pp.55-56
13. Kikuchi, M , Miyamoto, H. , Otoyoy, B and Kuroda, M (1991); JSME International Journal Series I, Vol.34 , No. 1, pp.90-97